The International Archives of the Photogrammetry, Remote Sensing and Spatial Information Sciences, Volume XLIX-B2-2026
XXV ISPRS Congress 2026 “From Imagery to Understanding”, Commission II, 4–11 July 2026, Toronto, Canada

Non-Contact Modal Analysis of Wind Turbine Blades Using Terrestrial Laser Scanner

Martina Goering

Jade University of Applied Sciences, Institute of Applied Photogrammetry and Geoinformatics (IAPG),
Ofener Str. 16/19, 26121 Oldenburg, Germany - martina.goering@jade-hs.de

Keywords: TLS, profile mode, wind turbine, rotor blade, eigenfrequencies, modal shapes.

Abstract

This contribution presents a methodology for non-contact, marker-free modal analysis of wind turbine blades using terrestrial laser scanning (TLS). The approach aims to determine key modal properties, such as natural frequencies and mode shapes, which are essential for assessing structural behaviour and service life. The methodology is systematically evaluated using simulated data, laboratory experiments, and full-scale field measurements. Simulations are used to analyse the influence of measurement noise and sampling rate, demonstrating that dominant frequencies can be identified with an accuracy of approximately 0.1 Hz. In addition, the first two bending mode shapes are reliably reconstructed, confirming the robustness of the segment-based processing workflow. In laboratory experiments, TLS and photogrammetry are used to capture vibrations of a 4 m long test object. Photogrammetric data, based on 3D coordinates of circular markers, serve as a reference for frequency identification using Fast Fourier Transform (FFT). TLS data are processed segment-wise, consistent with the field application, and show good agreement with the reference measurements. The method is subsequently applied to a full-scale rotor blade (88 m) in a field experiment. TLS profile measurements are transformed into a blade-aligned coordinate system and analysed to determine eigenfrequencies and mode shapes along the blade span. The results demonstrate that TLS enables reliable identification of dominant modal properties and provides a cost-effective alternative to conventional sensor-based approaches, with strong potential for practical applications in wind turbine monitoring.

1. Introduction

Wind turbine blades are typically designed for a service life of around 20–25 years (IEC, 2019). To extend this service life, a thorough understanding of the dynamic behaviour of the rotor blades is essential. This knowledge enables accurate fatigue analyses, improved structural health monitoring, and optimized maintenance strategies, all of which are critical for maximizing turbine efficiency and safety over extended service periods. A key factor for these analyses is precise knowledge of the blades modal parameters – their natural frequencies (eigenfrequencies) and corresponding vibration patterns (mode shapes).

However, accurately modelling these properties is challenging due to uncertainties in geometry, material properties, damping, and operational/environmental conditions. This frequently results in overly conservative safety margins, limiting the full exploitation of a turbine’s residual lifespan (Mozafari et al., 2024, Nielsen & Sørensen, 2021). Traditional experimental modal analysis (EMA), which requires extensive measurements with multiple accelerometers, is cumbersome and only performed for certification reasons (Gundlach et al., 2020, Luczak et al., 2021). Conducting EMA on operational wind turbines is costly, time-consuming, and necessitates long downtimes. In many practical applications, a reliable estimate of the dominant global dynamic behaviour – particularly the first two eigenfrequencies – often suffices (Stanoev & Chandrashekhara, 2019). These frequencies are associated with characteristic vibration patterns, or eigenmodes, in which the blade naturally bends in recurring, well-defined shapes. The first mode usually corresponds to the primary bending of the blade, while the second mode introduces additional variations in amplitude along the blade span.

A contactless alternative is Terrestrial Laser Scanning (TLS), which can capture structures marker-free from a distance. TLS-based frequency identification has already been demonstrated successfully for bridges (Meyer et al., 2023) and tower structures (Paffenholz et al., 2008), using high-frequency 2D profile scans. Transferring these approaches to rotor blades requires adaptations due to slender geometries, typically small amplitudes, and specific measurement geometries.

The aim of this work is to develop and validate a TLS-based workflow for identifying the main modal parameters of stationary rotor blades using 2D profile scans (Figure 1). The primary focus is on determining the first two eigenfrequencies. The corresponding mode shapes will be sketched in simplified form where feasible. For validation, simulations-driven and controlled laboratory investigations are conducted first, followed by a field campaign on the rotor blade. The field-specific reference data come from an EMA-based field investigation, whose procedures and results are described in Rosemeier et al. (2025). For confidentiality reasons, detailed measurement results are not published. Instead, deviations from the reference values and the standard deviations are presented.
This work combines simulation, laboratory tests, and field measurements to systematically validate a distance-based modal screening of rotor blades. The methodology describes challenges in data acquisition, profile extraction, and frequency identification, and the results are discussed with respect to practical applications and future monitoring or maintenance. The paper is organized as follows: first, the methodology is described and validated; next, results from simulations, laboratory tests, and a field experiment are presented. This is followed by a discussion of the findings and finally, a summary and outlook conclude the paper.

2. Method

This chapter presents the implementation of a TLS-based workflow for identifying the dominant modal parameters of rotor blades. The focus is on determining the first two natural frequencies and providing an initial characterization of the corresponding mode shapes. The approach integrates numerical simulations, laboratory experiments, and field measurements into a coherent and reproducible evaluation procedure. Data processing is carried out using the same software applied to the

This contribution has been peer-reviewed.

real TLS measurements, ensuring consistency between simulated and experimental results.

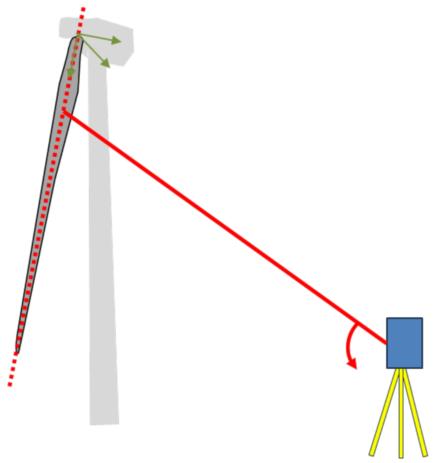

Figure 1. The laser scanner scans the rotor blade in profile mode.

2.1 Suitability of TLS

For rotor blades, Terrestrial Laser Scanning (TLS) must account for slender geometries, limited measurement setups, and relatively small vibration amplitudes. Direct point-to-point comparisons between profiles are not feasible because the blade moves, so each point does not occupy the same position in consecutive measurements. To overcome this, the blade is divided into segments along its longitudinal axis, and all measurements within each segment are averaged. This segment-based approach ensures that the relevant portions of the blade are consistently analysed, reduces the influence of noise, and allows a dominant frequency to be assigned to each section.
TLS has been successfully validated for bridges (Meyer et al., 2023), where the first natural frequency could be determined with an accuracy of approximately ±0.1 Hz and vibration amplitudes as small as 0.3 mm were detectable. Applied to rotor blades, expected dominant frequencies are up to 10 Hz, with amplitudes of up to 500 mm. To capture these vibrations reliably, TLS should operate in 2D mode with a sampling rate of at least 20 Hz. This workflow provides a robust method for identifying modal properties while accommodating the specific challenges of slender, flexible rotor blades.

2.2 Data Acquisition and Processing

Measurements are performed in profile mode. The TLS is positioned on the ground in front of the wind turbine and aligned as accurately as possible along the rotor blade longitudinal axis. Due to the distance and orientation, slight misalignments are inevitable, which can influence the apparent scanner alignment. Each 3D point is assigned a timestamp based on the fixed measurement frequency.

To analyse the blade dynamics, the profile coordinates are transformed into a blade-aligned object coordinate system. The longitudinal axis of the blade (Z-axis) is defined by fitting a straight line to measurements from the stable region near the blade root, ensuring a consistent representation of the blade span from root to tip. The Y-axis is oriented toward the TLS and is perpendicular to the Z-axis, while the X-axis completes the right-handed coordinate system.

The blade is divided along its span into discrete segments. For each segment, the mean displacement per profile is calculated using all points within a positional tolerance, producing time-dependent displacement signals for each segment.

Dominant frequencies are identified via a Fast Fourier Transform (FFT) applied to the segment signals, with parabolic interpolation used to refine peak frequency estimates. Based on these frequencies, mode shapes of the rotor blade are extracted by applying narrowband filters around each dominant frequency. Both amplitude and phase are preserved during this procedure, allowing correct identification of nodal points (zero crossings) along the blade.

The resulting mode shapes are referenced to the blade root (set to zero) and optionally smoothed to reduce noise effects. Mode amplitudes are normalized either individually per mode or with respect to the global maximum amplitude. The same computational workflow is applied consistently to both simulated and field data, ensuring comparability.

2.3 Validation

The workflow is validated through three complementary approaches: numerical simulation, laboratory experiments, and field measurements.

Simulation: The rotor blade is represented as a thin line along its longitudinal axis, and multiple vibration modes are superimposed to create a realistic motion. Simulated data are transformed into the TLS coordinate system to ensure the same processing workflow as used for field measurements. Input parameters include the number of modes, their frequencies, and simulated TLS-type noise to mimic measurement conditions.

Laboratory Experiments: A long, slender test object is excited into vibration, and reference data are collected photogrammetrically using circular markers (3D coordinates with timestamps). TLS measurements are recorded in parallel and processed using FFT analysis. Comparison of TLS and reference data allows validation of the identified frequencies.

Field Measurements: TLS data acquisition on the rotor blade follows the workflow described above. Reference data are obtained from an EMA-based field study (Rosemeier et al., 2025). Since the TLS and reference data were not recorded simultaneously, direct point-by-point comparisons are not possible. Detailed measurement results are not disclosed due to confidentiality constraints.

3. Results

This chapter presents the results obtained from simulations, laboratory experiments, and field measurements, highlighting the validation of the TLS-based workflow for rotor blade modal analysis.

3.1 Simulation

The TLS-based workflow was evaluated using simulated rotor blade data/clamped beam to assess its accuracy and robustness under controlled conditions. The simulation provides a reference dataset for testing segment-based frequency identification and mode shape reconstruction. The reference frequencies of the first two bending modes of the rotor blade are approximately 0.5 Hz and 3.5 Hz. The simulation used realistic measurement parameters: a rotor blade length of 86 m, 2,000 points per profile, a profile acquisition rate of 100 Hz, a total measurement duration of 10 s, and the first two bending modes superimposed. TLS-type random noise was added with standard deviations ranging from 0 mm to 100 mm to evaluate the influence of measurement noise. Maximum blade deflections were approximately 1 m.

Figure 2 illustrates a representative simulated rotor blade profile at a given time step, showing the point distribution along the span, the overall deformation, and the applied TLS-type noise (σ = 20 mm). This provides a visual impression of the measurement conditions and the relative magnitude of signal and noise.

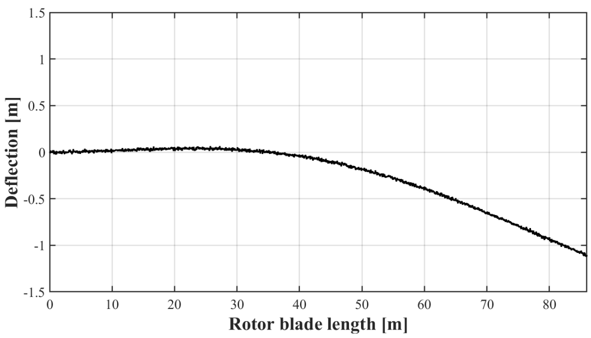

Figure 2. Simulated rotor blade profile at a representative time step, showing point distribution, maximum deflection (~1 m), and TLS-type noise (σ up to 20 mm).

Time-dependent displacement signals were analysed segment-wise using a Fast Fourier Transform (FFT) to identify dominant frequencies. Parabolic interpolation of the FFT peaks improved frequency accuracy, reducing deviations from the reference frequencies to the order of a few hundreds of a hertz. Identified frequencies were consistent across all segments, demonstrating the robustness of the segment-based approach. Even at high noise levels of up to 100 mm, the dominant frequencies were reliably identified, with standard deviations across segments below 0.0005 Hz, indicating negligible influence of measurement noise.

The influence of the profile acquisition rate on frequency identification was evaluated by comparing the identified frequencies to the reference values. At 32 Hz, deviations were negligible. Reducing the rate to 15 Hz, 10 Hz, and 8 Hz resulted in slightly larger deviations, with maximum deviations on the order of 0.003–0.005 Hz for the first mode and 0.001–0.003 Hz for the second mode. These results indicate that, while the method remains robust, lower sampling rates slightly reduce frequency accuracy.

Mode shapes were reconstructed by filtering the segment signals around the identified dominant frequencies, preserving both amplitude and phase information to ensure correct identification of nodal points along the blade. The resulting mode shapes were referenced to zero displacement at the blade root, optionally smoothed to reduce noise effects, and normalized either individually per mode or relative to the global maximum amplitude. Figure 3 presents the extracted first (blue) and second (red) bending modes along the blade span. In the first mode, the blade bends mainly at the tip. In the second mode, one point along the blade, about one-third from the root, hardly moves, which is typical for a blade held fixed at its root. Both modes retain their characteristic shapes despite the presence of measurement noise.

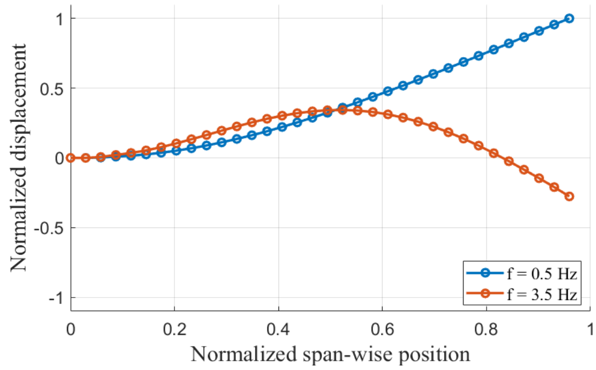

Figure 3. Extracted mode shapes along the blade: first (single antinode at tip) and second mode (one nodal point). Displacements normalized and referenced to blade root.

Overall, the simulation demonstrates that the proposed workflow provides reliable identification of both modal frequencies and spatial mode shapes. The method is robust to measurement noise and point density, while retaining sufficient sensitivity to capture the relevant dynamic behaviour of the rotor blade. The simulation thus provides a solid reference for subsequent laboratory and field validations.

3.2 Laboratory Experiment

Laboratory tests were conducted using a 4 m long test object fixed at one end to evaluate the TLS-based workflow under controlled conditions (Harms, 2024). Six vibration tests were performed, with the object manually excited at different locations to engage various segments. In tests 1–3, excitation occurred at the lower end, producing maximum deflections in that region. In tests 4–6, the excitation was varied to engage other parts of the object. Frequencies and amplitudes were determined at the positions of largest motion. The experimental setup is shown in Figure 4.

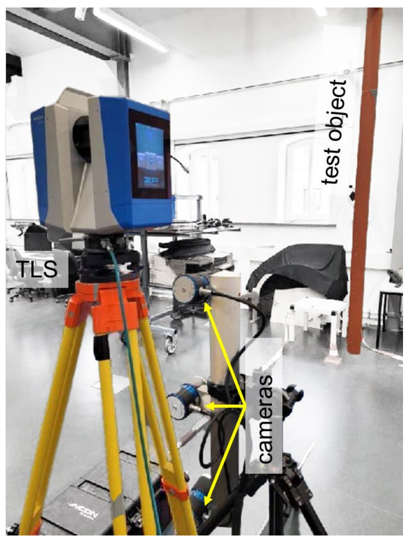

Figure 4. Laboratory experiment setup with TLS and photogrammetric reference markers (adapted from Harms, 2024).

Several tests were performed. In tests 1–3, the object was excited at its lower end, producing maximum deflections in that region. Frequencies and amplitudes were determined at the positions of maximum deflection. For tests 4–6, the excitation method was varied to compare different segments along the object.

Test	TLS Amplitude	TLS Frequency	Reference Amplitude	Reference Frequency
	mm	Hz	mm	Hz
1	260	0.39	300	0.36
2	450	0.42	480	0.36
3	780	0.41	790	0.36
4	100	1.27	90	1.33
5	130	1.68	120	1.75
6	130	3.80	120	3.86

Table 1. Measured amplitudes (mm) and frequencies (Hz) of six laboratory tests for TLS and photogrammetric reference measurements. TLS values were obtained by segment-wise averaging along the object.

The results are summarized in Table 1, showing both amplitudes and identified frequencies for TLS and photogrammetry. For tests 1–3, the TLS measured an average frequency of 0.40 Hz with deviations up to 0.06 Hz (standard deviation ±0.1 Hz). The AICON MoveInspect reference consistently recorded 0.36 Hz at the lowest marker, resulting in a TLS-to-reference deviation of 0.04 Hz. For tests 4–6, maximum deviations between TLS and MoveInspect were 0.07 Hz. Amplitude differences are primarily due to TLS segment averaging. Overall, TLS reliably reproduced the measured frequencies.

3.3 Field experiment

The field experiment was conducted on a wind turbine of the type Adwen AD 8-180, with a rotor blade length of 88 meters and a hub height of 115 meters. The rotor blade was fixed in the 6 o'clock position. The TLS was positioned such that its profile scan aligned with the longitudinal axis of the rotor blade, enabling the acquisition of cross-sectional profiles along the blade span (Figure 5).

Figure 5. Measurement setup for the field experiment showing the TLS and rotor blade orientation.

To induce measurable vibrations for the modal analysis, the rotor blade was manually excited by an operator standing on the blade platform. Data acquisition was performed at a frequency of 32 Hz in 2D mode, from a distance of 150 meters and an incidence angle of 40°, with a measurement rate of 250 kHz.

3.3.1 Data Preprocessing

The collected 3D coordinates (x, y, z) and timestamps were transformed into the rotor blade object coordinate system. The blade was divided into segments along its longitudinal axis, with each segment spanning ±0.5 m around the nominal positions of interest. Due to the closer proximity of the TLS near the blade tip, the number of points per segment increases toward the tip (see Figure 6). Segment-wise averaging was applied to reduce measurement noise and ensure consistent representation of each section.

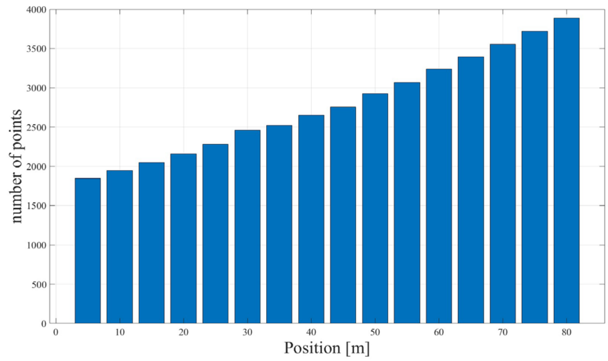

Figure 6. Division of rotor blade data into segments. The point density increases toward the blade tip.

TLS data were evaluated at 2.5 m intervals along the blade span. For each position, all points within the corresponding segment were averaged, and segment-wise FFT analysis was performed. Based on these results, the local modal amplitudes and mode shapes were determined for each segment, providing a detailed representation of the rotor blade’s dynamic behaviour.

Figure 7 shows example profile data from two segments (70 m and 80 m) during manual excitation. Only two areas are displayed to illustrate differences in vibration amplitude between segments.

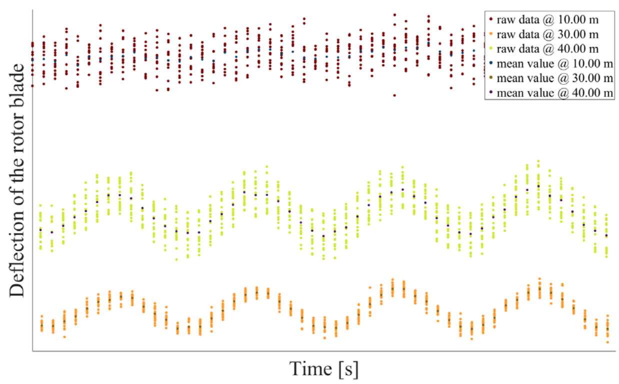

Figure 7. Example profile data from two segments (70 m and 80 m) during manual excitation.

3.3.2 Frequency Analysis

Segment-wise FFT analysis revealed significant vibrations along the rotor blade. Frequencies can be determined at multiple positions along the blade span, providing a spatially resolved representation of the dynamic behaviour. In Figure 8, results are shown for segments spaced at approximately 10 m intervals.

Vibrational amplitudes increase towards the blade tip, while lower amplitudes are observed near the root.

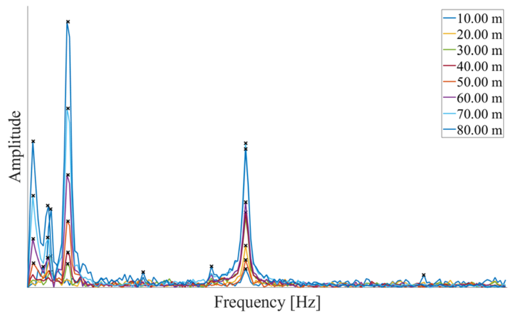

Figure 8. Calculated dominant frequencies and amplitudes for each segment of the rotor blade.

In addition to the blade-related frequencies, a pronounced low-frequency component is observed on the left side of the spectrum, which can be attributed to the natural frequency of the wind turbine tower.

For each segment, the FFT enabled identification of multiple frequency peaks and their corresponding standard deviations. In addition to the blade-related eigenfrequencies, further peaks are observed, including components related to the manual excitation. The dominant structural frequencies of the rotor blade can be clearly distinguished from these excitation-induced components. All identified eigenfrequencies exhibit standard deviations below 0.02 Hz, indicating a low noise level in the TLS measurements.

Reference measurements by the Fraunhofer Institute for Wind Energy Systems (IWES) using a modal hammer and accelerometers (Rosemeier et al., 2025) show deviations of less than 0.1 Hz compared to the TLS results. Although the measurements were not simultaneous, these results demonstrate that TLS can reliably determine rotor blade frequencies in the field.

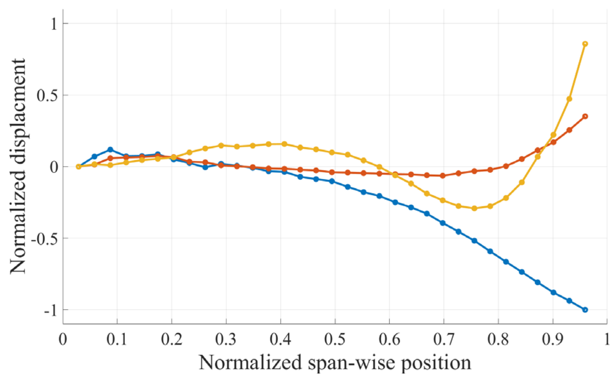

Figure 9. Normalized mode shapes of three eigenfrequencies along the rotor blade. Mode shapes are referenced to the blade root and smoothed.

3.3.3 Mode Shapes

Mode shapes were extracted from the measured signals using the identified dominant frequencies. Due to the profile-based TLS acquisition, mode shapes can be determined continuously along the blade span, allowing a detailed spatial representation of the deformation. The first three dominant mode shapes were successfully extracted along the blade span (Figure 9).

The mode shapes are referenced to the blade root, which is assumed to be fixed (zero displacement), and are normalized with respect to the maximum displacement along the blade. The blade length is represented in normalized form root to tip.

The TLS-derived mode shapes show very good agreement with reference data from the Fraunhofer Institute for Wind Energy Systems (IWES), confirming the suitability of TLS for field-based modal analysis.

4. Discussion

The simulations provide an ideal reference scenario, demonstrating that the segment-based FFT and modal extraction correctly identify the reference frequencies and mode shapes. Frequency deviations are minimal (<0.01 Hz), confirming the workflow ability to resolve small differences and establish a baseline for experiments.

TLS measurements of the 4 m test object were compared with photogrammetric reference data. Frequency deviations were up to 0.07 Hz, consistent with previously reported accuracy of 0.1 Hz (Meyer et al., 2023). Differences arise from segmentation and sampling rate differences. Amplitude discrepancies can be attributed to the spatial distribution of excitation and the segment-based averaging. Mode shapes were not derived for the laboratory experiment, as the focus was placed on frequency validation. However, the inclusion of mode shape reconstruction would enable a more direct comparison with the photogrammetric reference data and provide a more comprehensive validation of the TLS-based workflow.

Full-scale rotor blade measurements were compared with reference data from the Fraunhofer Institute for Wind Energy Systems (IWES) (Rosemeier et al., 2025) as well as manufacturer-specified frequencies. TLS-derived frequencies deviate by less than 0.1 Hz from the reference, showing that the method works reliably in the field. It should be noted that the TLS and IWES measurements were not acquired simultaneously, and a temporal offset between the datasets may influence the comparability of the results.

Manual excitation introduces variability in amplitude, but the first two bending modes are clearly and consistently captured. Additional, less dominant frequencies can also be identified in the TLS data, which are consistent with both IWES measurements and the nominal frequencies of the rotor blade, although with reduced peak prominence.

The transformation into a blade-aligned object coordinate system proved essential for the analysis. Without this transformation, the dominance of the spectral peaks is reduced, highlighting the importance of proper preprocessing for accurate frequency identification.

5. Conclusion and Outlook

Terrestrial laser scanning (TLS) has proven to be a reliable method for capturing the dynamic behavior of rotor blades. Simulations demonstrate that segment-based FFT and modal extraction accurately resolve reference frequencies and mode shapes along the blade, providing a solid reference for experimental validation.

https://doi.org/10.5194/isprs-archives-XLIX-B2-2026-175-2026 |

Laboratory experiments with a 4 m test object show that TLS measurements agree with photogrammetric reference data within 0.07 Hz, confirming the method’s accuracy for controlled setups. Full-scale field measurements on an 88 m rotor blade further validate TLS capabilities, with frequency deviations of only 0.05 Hz relative to IWES reference data. Proper preprocessing, including transformation into the blade object coordinate system and segment-based averaging, is crucial for correctly identifying mode shapes.

Future work will focus on integrating photogrammetric data acquired with black circular markers during the field experiment, which could provide an additional comparison and cross-validation of TLS-derived frequencies and mode shapes. Incorporating spatio-temporal models may also enhance the consistency and resolution of modal analysis along the blade. In addition, the potential for capturing torsional behaviour of rotor blades using two terrestrial laser scanners operating in profile mode will be investigated. A slight temporal offset between the systems would be required to avoid interference during distance measurements. Such a setup could enable the estimation of torsional deformation in addition to bending modes.

Overall, TLS offers a non-intrusive, high-resolution approach for wind turbine rotor blade monitoring, with potential for widespread application in both laboratory and field environments.

Acknowledgements

Acknowledgements are given to the German Federal Ministry for Economic Affairs and Energy (BMWE) for supporting the BLADAPTION project (03EE3086A, 03EE3086B). The author thanks the photogrammetry working group at the IAPG for valuable feedback and discussions. Further appreciation is extended to the IWES for providing reference measurement data used for validation. Further appreciation is extended to Siemens Gamesa Renewable Energy Deutschland GmbH for providing a wind turbine for field measurements, and to Zoller + Fröhlich GmbH for providing the laser scanner Z+F Imager 5016 used in this research.

References

Harms, F., 2024: Untersuchungen zur Laserscanner-basierten Schwingungsmessung am Beispiel eines Rotorblattes einer Windenergieanlage im Stillstand. Unpublished master's thesis. Jade University of Applied Sciences, Oldenburg, Germany.

IEC, 2019: IEC 61400-1: Wind energy generation systems – Part 1: Design requirements. International Electrotechnical Commission, Geneva.

Luczak, M. M., Riva, R., Yeniceli, S. C., Madsen, S. H., Di Lorenzo, E., 2021: Identification of the test setup influence on the modal properties of a short wind turbine blade during fatigue test. Measurement, 174, 108960. doi.org/10.1016/j.measurement.2020.108960

Meyer, N., Schmid, L., Wieser, A., Medic, T., 2023: Vibration monitoring of a bridge using 2D profile laser scanning: Lessons learned from the comparison of two spatio-temporal processing strategies. In: 5th Joint International Symposium on Deformation Monitoring (JISDM 2022), 177–184.

Mozafari, S., Veers, P., Rinker, J., Dykes, K., 2024: Sensitivity of fatigue reliability in wind turbines: Effects of design turbulence and the Wöhler exponent. Wind Energy Science, 9, 799–820. doi.org/10.5194/wes-9-799-2024

Nielsen, J., Sørensen, J., 2021: Risk based derivation of target reliability levels for life extension of wind turbine structural components. Wind Energy, 24(9), 939–956. doi.org/10.1002/we.2610

Paffenholz, J. A., Vennegeerts, H., Kutterer, H., 2008: High frequency terrestrial laser scans for monitoring kinematic processes. UNGEO 2008 – 4th International Conference on Engineering Surveying, 23–24.

Rosemeier, M., Göring, M., Horstmann, T., Kranz, M., 2025: Field experimental modal analysis of an 88.4 m wind turbine rotor blade. Wind Energy Science Conference, France.

Stanoev, E., Chandrashekhara, S. K., 2019: Determination of natural frequencies and mode shapes of a wind turbine rotor blade using Timoshenko beam elements. Wind Energy Science, 4, 57–69. doi.org/10.5194/wes-4-57-2019